AALBORG UNIVERSITY

DENMARK

Fuzzy droop control loops adjustment for stored energy balance in distributed energy storage system

Aldana, Nelson Leonardo Diaz; Wu, Dan; Dragicevic, Tomislav; Quintero, Juan Carlos Vasquez; Guerrero, Josep M.

Fuzzy Droop Control Loops Adjustment for Stored Energy Balance in Distributed Energy Storage System

Nelson L. Díaz*†, Dan Wu*, Tomislav Dragičević*, Juan C. Vásquez*, Josep M. Guerrero*

* Department of Energy Technology, Aalborg University, Aalborg, Denmark.
†Faculty of Engineering, Universidad Distrital F. J. C., Bogotá, Colombia.
nda@et.aau.dk, dwu@et.aau.dk, tdr@et.aau.dk, juq@et.aau.dk, joz@et.aau.dk
www.microgrids.et.aau.dk

Abstract—**The study of isolated AC microgrid has been under high interest due to the integration of renewable energy resources especially for remote areas, or to improve the local energy reliability. The current trend is oriented to distributed renewable energy sources and their corresponding energy storage system, in order to smooth the variations at the prime energy generator. In this paper, a decentralized strategy based on fuzzy logic is proposed in order to balance the state of charge of distributed energy storage systems in low-voltage three phase AC microgrid. The proposed method weights the action of conventional droop control loops for battery based distributed energy storage systems, in order to equalize their stored energy. The units are self-controlled by using local variables, hence, the microgrid can operate without communication systems. Frequency and voltage bus signaling are used in order to coordinate the operation of the microgrid under different stages for charging batteries. Simulation results show the feasibility of the proposed method.**

Keywords—Distributed energy storage systems, Droop control, Fuzzy inference system, State of charge.

I. INTRODUCTION

The integration of Renewable Energy Sources (RES) such as photovoltaic (PV) and wind turbine generators (WTG), in order to use clean and renewable energy instead of traditional coal, oil and other non-renewable energy resources, has been under rapid development in the world nowadays. A microgrid appears as an effective solution for interconnecting RES, energy storage systems (ESS) and loads as controllable entities, which may operate in grid-connected or islanded mode, either in AC or DC configuration [1], [2]. Particularly, islanded microgrids play and important role when economic and environmental issues do not allow an interconnection with the main grid [1], [3]. Indeed, isolated microgrids become an additional challenge since the voltage and frequency are not imposed for the main grid. Therefore, every distributed energy resources has to cooperate in order to ensure the reliability, security and power stability of the local grid [4], [5].

However, the intermittent nature of RES, added together with unpredictable load fluctuations, may cause instantaneous power unbalances that affect
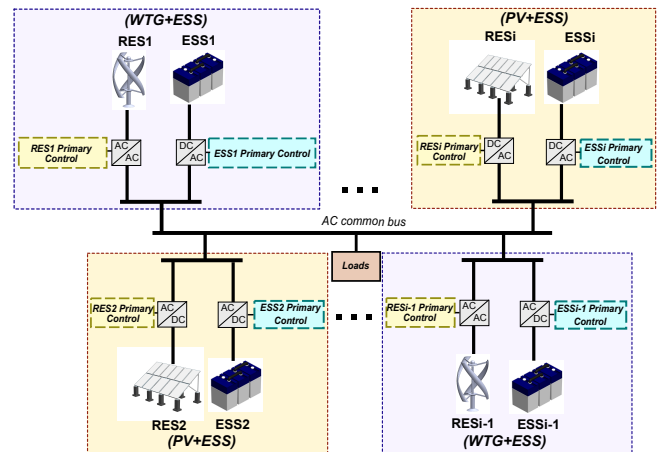

Figure 1: Islanded AC microgrid configuration based on distributed (PV+ESS) and (WTG+ESS) generators.

the operation of the microgrid. Hence, ESS are required for ensuring the operating conditions of the power grid by smoothing the variations of RES [6]–[8]. In fact, there are two ways of integrating ESS (aggregated or distributed) [9], [10]. At this sense different studies have been done in order to compare the performance of these two strategies. In general, some results show advantages in the distributed strategy [9]. Anyhow, the current trend is oriented to distributed ESS where an ESS is associated to its corresponding RES into an entity denoted as active generators (PV+ESS or WTG+ESS), as is shown in Fig. 1. This configuration, aims to ensure constant power production when PV and WTG are used [6], [8], [11], [12], . Commonly, in islanded microgrids the ESS are composed of banks of valve regulated lead-acid (VRLA) batteries [1], [13]–[15].

When a microgrid is composed by distributed ESS, a coordination to ensure stored energy balance between the units is required. This coordination aims to avoid deep-discharge in one of the ESS and over-charge in the others. Consequently, during the charging process, it is desirable to prioritize the charge of the unit with the smallest state of charge (SoC), and similarly, during the discharging process,

the unit with the highest SoC should provide more power to the microgrid than the others in order to ensure stored energy balance [16]–[18]. Commonly, droop control strategies are used in order to achieve power sharing between units. Therefore, conventional control loops for power sharing at each ESS are complemented with stored energy balance control actions which adjust the droop coefficients in accordance to the SOC.

Different approach based on centralized and distributed strategies have been proposed for energy storage balance in distributed ESS for DC microgrids [13], [15], [19]–[22]. The main drawback of those strategies is that they are based on centralized control units, and they require the use of communication systems, which are not always suitable for decentralized configurations of a microgrid. A decentralized method for a DC microgrid has been proposed in [23] which does not use communication between units. However, in [23] the authors only consider the equalization process when the batteries are under discharge. In [24] authors consider a double quadrant method for DC microgrids which ensure SOC equalization for both charging and discharging process. Even so, those methods require the knowledge of the initial SoC at each unit in order to obtain adequate values for their parameters, and for ensuring the stability of the system. In the same way, in [25] a decentralized adaptive droop control have been proposed for equalizing the SoC of distributed ESS in DC microgrid. Nevertheless, in [25] it is required a previous knowledge about the characteristics of the others ESS in order to calculate the charge and discharge functions. On top of that, a strategy based on a fuzzy inference systems (FIS) was proposed previously for islanded DC microgrids [16]. This strategy assures good stored energy balance, and additionally it is absolutely modular, expandable. Indeed, centralized control and communications between units are not required. Another important issue to take into account, is that the proposed strategy takes into account the different stages required for charging an ESS based on batteries. Apart from that, it is important to consider how the battery charge process is coordinated with the operation of the others distributed energy resources into an islanded microgrid.

In this paper, the FIS proposed in [16] is adapted, applied and evaluated for an islanded AC microgrid. In this case, the proposed FIS weights the $P - \omega$ droop coefficients of the droop controllers in accordance with the SoC at each ESS. In particular, the implementation of this strategy implies additional challenges in the primary control loops since the AC microgrid has to deal with issues associated with synchronization, reactive power flows, and DC/AC conversion losses, which are not a concern in DC microgrids [20].

This paper is organized as follows: Section II describes the operation of the islanded microgrid under different control operation modes. Section III shows the design and operations of the proposed fuzzy strategy for stored energy balance. Section IV explain how the droop control loop for each RES is adjusted in order to ensure power sharing proportional to their maximum power. Finally, section V presents simulation results under different operational conditions. The proposed method is tested in a low voltage AC microgrid under islanded operation. Simulation results based on a MATLAB/Simulink model of the microgrid are presented to show the applicability and advantages of the proposed strategy. Finally, Section VI presents conclusions and perspectives for future works.

II. ISLANDED MICROGRID OPERATION

Normally, in an islanded microgrid all the power converters operate in voltage control mode (VCM) by following conventional droop control strategy, aimed to regulate the bus voltage and frequency and achieve good power sharing between units [26]. Droop control, enhances system reliability, expandability, and ensures the robustness without the use of external communication system [5], [27]. This approach works well with dispatchable power sources such as diesel generators but it is not effective for intermittent sources such as RES which are more likely to operate under an algorithm of maximum power tracking (MPPT). At that case, RES units behave as current sources and operate on current control mode (CCM) [1], [5]. Meanwhile, the ESS operate in VCM being responsible of regulating the bus voltage. Then, under VCM the batteries will be charged or discharged in order to compensate the unbalance between the energy generated by RES and load consumption [16], [28].

However, the most effective way of charging a battery is by means of a two stages procedure which involve two different control loops [14]. First, the ESS are charged based on the energy unbalance between RES generation and load consumption, at this moment, the power is limited by droop control loops, then the ESS operate under VCM. Subsequently, when the voltage per cell reach a threshold value (V_r), known as the regulation voltage (typically 2.45 ± 0.05 volts/cell), the battery voltage should be kept constant and the current at the battery will approach to zero asymptotically, and once it falls below a certain value, the battery may be considered as fully charged [14], [29]. At this point, each ESS draws as much power as needed to keep its battery voltage at V_r [15]. Because of this, each ESS operates on CCM and the RES must assume the responsibility of bus voltage regulation. As a consequence, the RES change their operation mode to VCM. To be more precise, the primary control of each distributes energy resource is composed by two control loops (VCM and CCM) and they should be able switch between them as is shown in Fig. 2. In
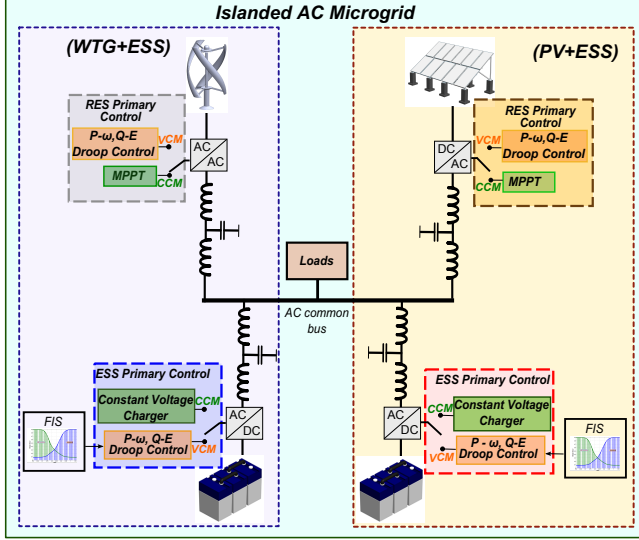
Figure 2: Islanded AC microgrid with (PV+ESS) and (WTG+ESS) generators.

light of the above, the operation of each RES and ESS in the microgrid should be accompanied by a decision-maker strategy in order to switch between controllers. Bus-signaling method, by using different bus voltage/frequency thresholds, is used to trigger the changes at the operation mode for RES and ESS in a coordinated way [5], [16].

At this paper in order to simplify the analysis an islanded microgrid composed by two RES (PV and WTG), loads, and two banks of valve regulated lead-acid (VRLA) batteries, as the one shown in Fig. 2, will be consider.

A. Reactive power sharing

Since voltage bus signaling will be used for determining the transitions between control modes at each distributed energy resource, reactive power $Q - E$ control loops play an important role. Conventional $Q - E$ droop controllers defined by the following equation:

$$E = E^* - n \cdot Q \tag{1}$$

are used in order to share equally the reactive power flow between units in a microgrid. In (1) E is the voltage amplitude in the common bus, Q is the reactive power at the respective unit, E^* is the voltage reference and n is the droop coefficient [27].

At this application only the units working under VCM are responsible of reactive power flow, for that reason they will establish the amplitude of the output voltage E in accordance to (1). To be more precise, ESS and RES units, interchange the responsibility of the reactive power flow. Since bus voltage-signaling is used for triggering the changes at the decision-makers, a positive droop coefficient (n) is defined for ESS and a negative droop coefficient (n) is defined for RES. In this way it is possible to
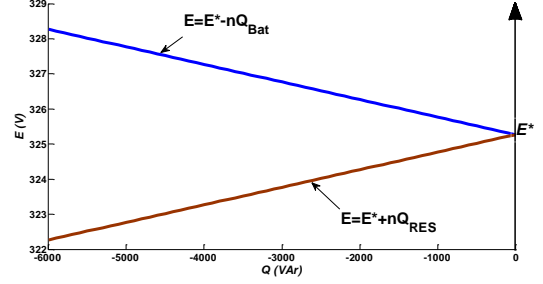

Figure 3: Droop characteristics $Q - E$

identify which one (ESS or RES) are operating under VCM. Equation (1) is redefined as:

$$E = \begin{cases} E^* - n \cdot Q_{Bati}, & \textbf{When } ESS \textbf{ are } in \ VCM; \\ E^* + n \cdot Q_{Resi}, & \textbf{When } RES \textbf{ are } in \ VCM. \end{cases} \tag{2}$$

where (Q_{Bati}) and (Q_{Resi}) represent the reactive power flow at each ESS and RES respectively. The droop coefficient n is calculated for a voltage deviation smaller than 5% at the common bus. Fig. 3 represents graphically the operation of the $Q - E$ droop control loop.

B. Decision-maker operation

Decentralized finite state machines with two states are used at each RES and ESS unit in order to coordinate the changes at the control operation mode. The transition between operation modes are triggered by bus voltage/frequency-signaling, the battery array voltage (V_{Bati}), and the power comparison when the MPPT value is smaller than the generated power for ESS and RES respectively. Fig. 4a shows the Moore finite state machine proposed for ESS, where the input variables are defined by the following equations:

$$X_{1Batt} = \begin{cases} 1, & \textbf{When } V_{Bati} \geq V_r; \\ 0, & \textbf{Otherwise} . \end{cases} \tag{3}$$

$$X_{2Batt} = \begin{cases} 1, & \textbf{When } freq_{ACbus} \leq frec_t; \\ 0, & \textbf{Otherwise} . \end{cases} \tag{4}$$

$$X_{3Batt} = \begin{cases} 1, & \textbf{When } E \geq E^*; \\ 0, & \textbf{Otherwise} . \end{cases} \tag{5}$$

where $freq_{ACbus}$ is the frequency at the common bus, and $freq_t$ is the threshold frequency.

Likewise, Fig. 4b shows the Moore finite state machine established for RES, and the input variables are defined by the following equations:

$$X_{1RES} = \begin{cases} 1, & \textbf{When } freq_{ACbus} \leq frec_t; \\ 0, & \textbf{Otherwise} . \end{cases} \tag{6}$$

$$X_{2RES} = \begin{cases} 1, & \textbf{When } E \geq E^*; \\ 0, & \textbf{Otherwise} . \end{cases} \tag{7}$$
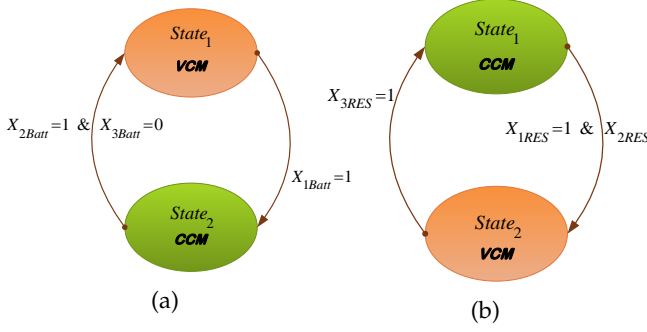
(a)   (b)

Figure 4: Finite state machines for: (a) ESS Decision-maker (b) RES Decision-maker.

$$X_{3RES} = \begin{cases} 1, & \textbf{When } P_{MPPT} < P_{RESi}; \\ 0, & \textbf{Otherwise} . \end{cases} \quad (8)$$

where P_{MPPT} is the power reference given by the MPPT algorithm, and P_{RESi} is the power generated for each RES unit.

III. Fuzzy adjustment for SoC balance

When batteries are in the process of charge or discharge, the power balance is managed by $P - \omega$ droop control loops [27]. Therefore, the frequency at the common AC bus given by the following equation:

$$\omega = \omega^* - m \cdot P_{Bati} \quad (9)$$

where m is the droop coefficient, ω is the angular frequency at the common bus, ω^* is the reference of the angular frequency, and P_{Bati} is the power driven at each ESS. If we consider differences in the droop coefficients (m) at each ESS, the battery with the lowest m will inject/extract more power to/from the grid in order to keep the power balance in the microgrid [2]. For that reason, the ESS with the lowest m will be charged or discharged faster than the other.

For energy storage equalization, it is desirable that the battery with the lowest SoC will be charged faster than all the others and in this way ensuring stored energy balance. Then, a smaller m should be assigned to that battery. Likewise, when batteries are supplying power to the microgrid, it is desired that a larger m is assigned to the battery with the lowest SoC, in order to prevent a deep discharge and balance the stored energy. Accordingly, the SoC can be equalized when correct values of m are assigned to each ESS. In addition, the value of m has to be adjusted when the different SoC's approach between them.

In particular, a FIS can easily summarize all the qualitative knowledge, expressed above, about the expected behavior of the system in order to weight the droop coefficient at each ESS based on its own SoC [16]. Therefore, a fuzzy weighting factor $W(SoC_{Bati})$ is proposed for weighting the droop coefficient as is shown in Fig. 5, where it is assumed
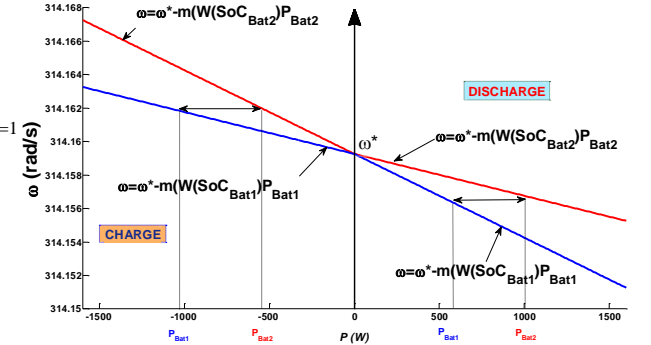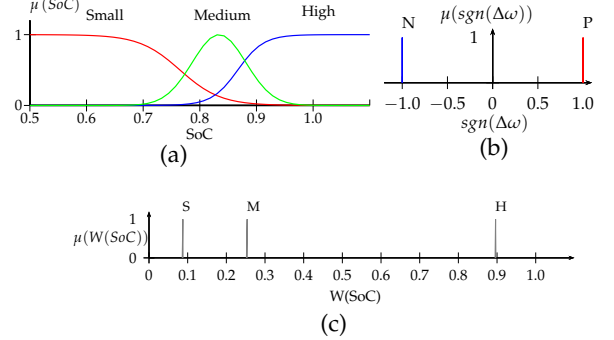

Figure 5: Droop characteristics $P - \omega$

(a)   (b)

(c)

Figure 6: Membership functions: (a) Input SoC, (b) Input $sgn(\Delta\omega)$, (c) Output $W(SoC)$.

$SoC_{Bat2} > SoC_{Bat1}$. As a result, equation (9) is rewritten as:

$$\omega = \omega^* - m \cdot W(SoC_{Bati}) \cdot P_{Bati} \quad (10)$$

Given the above points, a Mamdani FIS has been proposed in order to establish the weighting factor $W(SoC)$ at each ESS based on its corresponding SoC. This kind of FIS are usually used in feedback control mode, because they are computationally simple, present low sensibility to noise in the input, what is important in power system, and they can easily represent the knowledge about the expected control action [30]. The knowledge is represented by means of rules in the form *if-then* and synthesized in form of an input-output mapping between the antecedent and the consequent [30]. The consequent of the proposed FIS is the weighting factor $W(SoC)$, and the antecedents are the SoC and the sign of the frequency deviation ($sgn(\Delta\omega)$) defined by the following equation:

$$sgn(\Delta\omega) = \begin{cases} 1, & \textbf{If } \omega - \omega^* > 0; \\ -1, & \textbf{If } \omega - \omega^* < 0. \end{cases} \quad (11)$$

For the SoC three membership functions have been defined with the linguistic labels "*Small*", "*Medium*" and "*High*" as is shown in Fig. 6a. Likewise, for the $sgn(\Delta\omega)$ two singleton membership functions have been defined with the linguistic labels "*N*" and "*P*" (see Fig. 6b). Finally, for the output $W(SoC)$ three singleton membership function have been defined with the linguistic labels "*S*", "*M*" and "*H*" (see Fig. 6c).
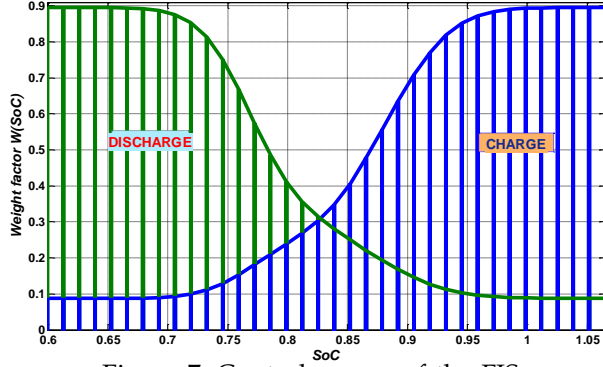
Figure 7: Control curves of the FIS.

To conclude, the proposed rule base is summarized as follows:

1. **If** *SoC* **is** *Small* **and** $sgn(\Delta\omega)$ **is** *N*
   then $W(SoC)$ **is** *H*

2. **If** *SoC* **is** *Small* **and** $sgn(\Delta\omega)$ **is** *P*
   then $W(SoC)$ **is** *S*

3. **If** *SoC* **is** *Medium* **and** $sgn(\Delta\omega)$ **is** *N*
   then $W(SoC)$ **is** *M*

4. **If** *SoC* **is** *Medium* **and** $sgn(\Delta\omega)$ **is** *P*
   then $W(SoC)$ **is** *M*

5. **If** *SoC* **is** *High* **and** $sgn(\Delta\omega)$ **is** *N*
   then $W(SoC)$ **is** *S*

6. **If** *SoC* **is** *High* **and** $sgn(\Delta\omega)$ **is** *P*
   then $W(SoC)$ **is** *H*

The SoC is estimated by ampere-hour (Ah) counting method [15],

$$SoC = SoC(0) - \int_0^t \frac{I_{bat}(\tau)}{C_{bat}} d\tau \qquad (12)$$

where $SoC(0)$ is the initial SoC, C_{bat} is the battery array capacity, and I_{bat} is the current of each battery. Fig 7 shows the control curve of the FIS. We can see from Fig. 6 and 7 that the droop coefficient *m* for each ESS will be weighted between 0.1 to 0.9 of its nominal value.

IV.   RES DROOP CONTROL LOOPS

As mentioned before, all the RES units change their operation mode to VCM once all the battery arrays reach the threshold voltage V_r. Despite, the droop control action described by equation (9) allows to share equally the active power flow between units, this is not practically possible when different RES are used in the microgrid. To be more precise, each RES unit has its own power rating and its own maximum power point. For that reason, it is not possible to ensure that all RES units can contribute equally on the power sharing. Therefore, the power contribution of each RES should be arranged in

Table I: Parameters of the Microgrid

Parameter	Symbol	Value
	Power Stage	
Nominal Bus Voltage	E^*	$230 * \sqrt{2}$ V
Nominal Bus Frequency	ω^*	$2 * \pi * 50$ rad/s
Inverter inductors	L	1.8mH
Filter Capacitor	C	27μF
Nominal Load	P_{Load}	1587 W
Maximum (RES) Power Rating	P_{RESmax}	2750 W
	Battery Array	
Nominal Voltage	$Vbat$	672 V
Regulation Voltage	V_r	756 V
Nominal Battery Capacity	C_{bat}	0.02 Ah
	Power flow Control	
$(P-\omega)$ Droop Coefficient	m	$1.25 * 10^{-5}$ (rad)/(s)/(W)
$(Q-E)$ Droop Coefficient	n	$5 * 10^{-4}$ V/(VAr))
Reactive power Reference	Q^*	0 VAr

accordance to its maximum power point. For that reason, a weighting factor $1000/P_{MPPTi}$ is applied to (9) then,

$$\omega = \omega^* - m \cdot \left(\frac{1000}{P_{MPPTi}} \right) \cdot P_{RESi} \qquad (13)$$

where P_{MPPTi} is the reference given by the MPPT algorithm for each RES, and P_{RESi} is the power supplied by each RES under VCM operation.

V.   SIMULATION RESULTS

A MATLAB/simulink model of the microgrid has been used in order to test and compare the performance of the microgrid with and without the use of the weighting factor $W(SoC)$. The microgrid is composed by a (PV+ESS) and a (WTG+ESS) generators as shown in Fig. 2. The microgrid has been designed to supply a nominal resistive load in a balanced three phase system. Detailed models of the VRLA battery arrays are used as proposed in [15], for simulating the batteries. A bank of batteries of $672V$ is used to ensure the nominal bus voltage with a modulation index around 0.9 in order to avoid over-modulation at the PWM signal. Table I summarizes the main characteristics of the microgrid.

Fig. 8 summarizes some results under changes at the power generated by RES. At this case, it is assume that the energy generated by both RES is the same and they change from $500W$ to $1500W$ at $Time = 10s$. An initial SoC of 75% for battery 1 ($Bat1$) and 85% for battery 2 ($Bat2$) has been established. At the top part of Fig. 8 (No Fuzzy Factor), we can see the voltage at the DC bus of each ESS (V_{Bat1} and V_{Bat2}), the power in the load (P_{Load}), the power at each RES (P_{Res1} and P_{Res2}), and the power at each ESS (P_{Bat1} and P_{Bat2}), when the fuzzy factor is not used. In the middle of Fig. 8 we can compare the SoC behavior with the fuzzy weighting factor (continuous line), and without the fuzzy weighting factor (dashed line). Finally, at the bottom of Fig. 8 (With Fuzzy Factor) we can see the voltage at the DC bus at each ESS (V_{Bat1} and V_{Bat2}), the power in the load (P_{Load}), the power at each RES (P_{Res1} and P_{Res2}) and the power at each ESS (P_{Bat1}
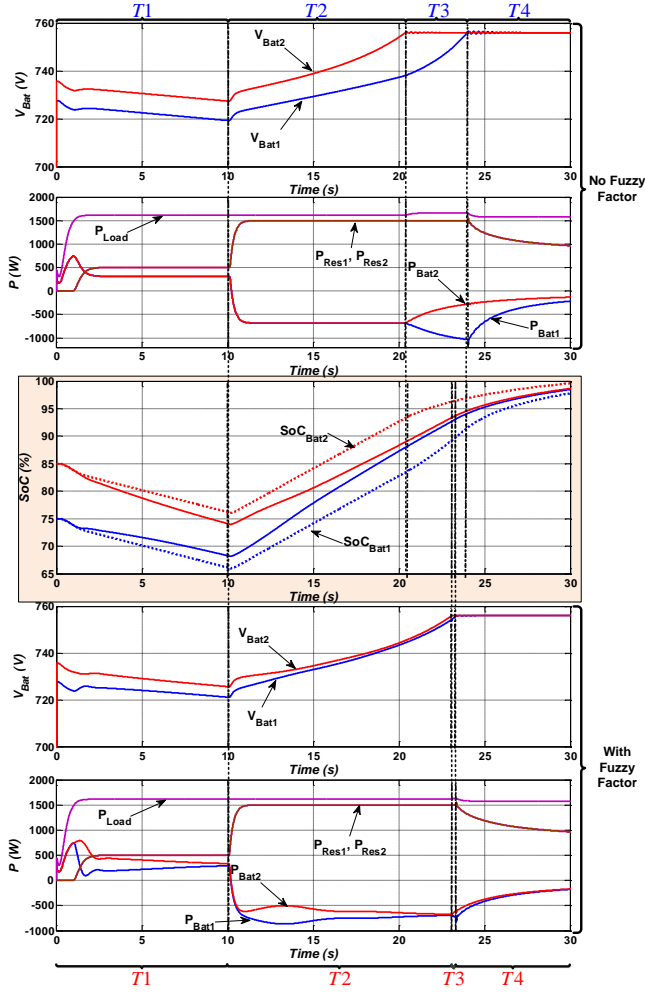
Figure 8: Simulation results with (bottom figures) and without (top figures) fuzzy factor

and P_{Bat2}), when the fuzzy factor $W(SoC)$ is used. The fuzzy factor is activated at $Time = 3s$.

Simulation time is split into 4 stages in order to indicate the changes at the operation mode of each RES and ESS. Table II summarizes the changes on the operation mode of each ESS and RES in accordance with times $T1$ to $T4$. We can see from Fig. 8 how the SoC of both ESS approach asymptotically one to the other. Additionally, it is possible to see that the system with fuzzy weighting factors reduces the depth of discharge at battery 1. Moreover, both batteries are charged faster taking into account that $T1 + T2 + T3$ is smaller when the fuzzy factor is used. Apart from that, the peak power of battery 1 is smaller in the system that uses the fuzzy weight factors. We can see after $T3$ and $T4$ that the voltage at the battery arrays is kept constant such as recommended in [14]. In $T4$ it is possible to see that both RES share power equally, since the same MPPT reference value is assumed for both RES.

Fig. 9 presents the behavior of the microgrid when two RES with different maximum power are used. At this case, only the operation with the fuzzy

Table II: Changes at the operation control mode for RES and ESS

	T1	T2	T3	T4
RES1	CCM	CCM	CCM	VCM
RES2	CCM	CCM	CCM	VCM
ESS1	VCM	VCM	CCM	CCM
ESS2	VCM	VCM	VCM	CCM

factor is considered. The changes at the control operation mode are also in accordance with Table II. For this case, it is assume that the MPPT reference for RES1 and RES2 are $500W$ and $250W$ respectively. At $Time = 10s$ the references values changes to $2000W$ and $1000W$ respectively for RES1 and Res2. Such as in the previous case, an initial SoC of 75% for battery 1 ($Bat1$) and 85% for battery 2 ($Bat2$) has been established. From Fig. 9, when the RES change their operation mode to VCM ($T4$), we can see that the power contribution of each RES is established in accordance to their maximum power point. As a matter of fact, RES1 contribute with more active power than RES2.
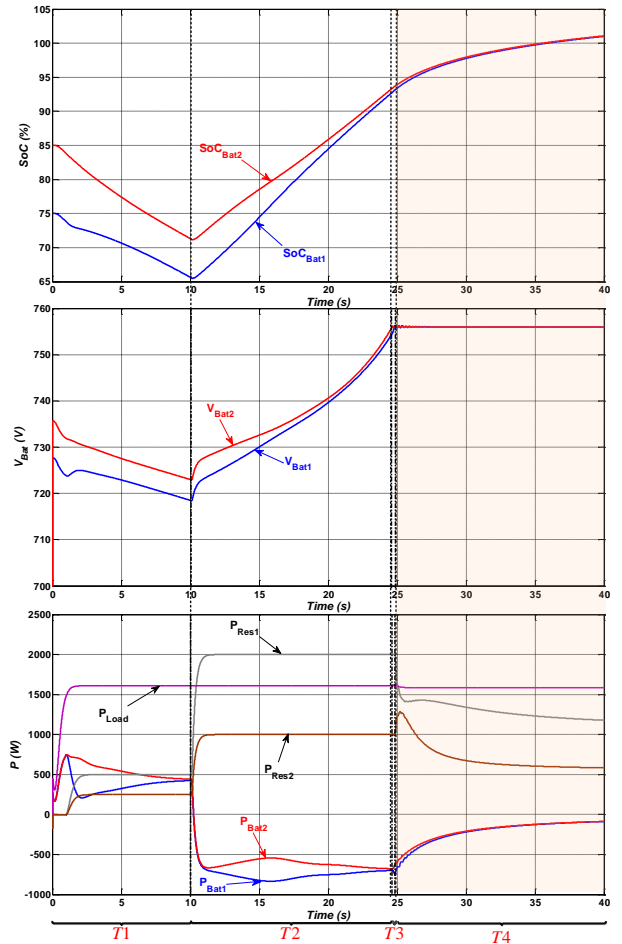

Figure 9: Simulation results with diferent P_{MPPT} at each RES

A more realistic scenario is presented in Fig. 10 in which the behavior of the microgrid is evaluated by emulating a single day. RES1 corresponds to a PV generator and RES2 corresponds to a WTG. At

Table III: Changes at the operation control mode during a day

	T1	T2	T3	T4
PV	CCM	VCM	CCM	CCM
WTG	CCM	VCM	VCM	CCM
ESS1	VCM	CCM	CCM	VCM
ESS2	VCM	CCM	CCM	VCM

this case, the maximum power at each RES change every hour by emulating the behavior of real PV and WTG in a day. The nominal power of each RES is $2750W$ and the battery capacity of each ESS has been set to $20(Ah)$. From Fig. 10 it is possible to see the fuzzy equalization process for the SoC during a day. Initial SoC of 85% for battery 1 ($Bat1$) and 95% for battery 2 ($Bat2$) has been defined. We can see that the SoC is completely equalized after 12 hours. On top of that, Table III summarizes the changes at the control operation mode for all the distributed energy resources in one day.

At the beginning ($T1$), RES units operate under MPPT, and the batteries are charged or discharged in accordance to the power unbalance between power generation and consumption. Meanwhile, distributed FIS balance the stored energy between batteries, and the SoC is equalized. At ($T2$) both batteries have reached the threshold voltage at the same time since the SoC has been equalized. At this point, all the distributed energy units change their operation mode as is shown in Table III. At the end of $T2$, the power reference given by the MPPT algorithm is smaller than the power supplied by the PV generator under VCM operation ($P_{MPPT} < P_{RES1}$). Because of this, RES1 changes its operation mode to CCM but RES2 continuous its operation under VCM during $T3$. Finally, at $T4$ RES2 changes its operation mode to CCM, since the reference given by the MPPT algorithm is smaller than the generated power. At the same time, both ESS change their operation mode to VCM, and they start to support the voltage regulation.

VI. CONCLUSIONS

The proposed adjustment of the droop coefficient by using a fuzzy inference system, ensures good storage energy balance for distributed ESS. Additionally, this strategy is absolutely modular, expandable, and it is not required a centralized control. As a matter of fact, it can be used directly when a new active generator has to be added to the microgrid without any modification. Likewise, the proposed method shows additional advantages compared to traditional methods such as asymptotic approximation of the SoC under process of charge and discharge, faster charge in the total of distributed ESS and reduction of the deep of discharge for the ESS with smallest initial SoC among others. Another advantage of the proposed FIS is that the same FIS can be applied to different values of droop coefficient and even more the same FIS

can be applied for AC or DC microgrids. On top of that, the microgrid can operate in a stable way under different scenarios without using communications. The use of decision making strategies at each distributed energy resource is required in order to ensure adequate transition between operation control mode and reliable operation.

REFERENCES

[1] J. de Matos, F. e Silva, and L. Ribeiro, "Power control in ac isolated microgrids with renewable energy sources and energy storage systems," *IEEE Transactions on Industrial Electronics,*, vol. PP, no. 99, pp. 1–1, 2014.

[2] J. Guerrero, J. Vasquez, J. Matas, L. de Vicua, and M. Castilla, "Hierarchical control of droop-controlled ac and dc microgrids a general approach toward standardization," *IEEE Transactions on Industrial Electronics*, vol. 58, no. 1, pp. 158–172, 2011.

[3] C. Wang, M. Liu, and L. Guo, "Cooperative operation and optimal design for islanded microgrid," in *2012 IEEE PES Innovative Smart Grid Technologies (ISGT)*, pp. 1–8, Jan 2012.

[4] M. Fazeli, G. Asher, C. Klumpner, L. Yao, and M. Bazargan, "Novel integration of wind generator-energy storage systems within microgrids," *IEEE Transactions on Smart Grid*, vol. 3, pp. 728–737, June 2012.

[5] D. Wu, F. Tang, T. Dragicevic, J. Vasquez, and J. Guerrero, "Autonomous active power control for islanded ac microgrids with photovoltaic generation and energy storage system," *IEEE Transactions on Energy Conversion,*, vol. 29, pp. 882–892, Dec 2014.

[6] H. Kanchev, D. Lu, F. Colas, V. Lazarov, and B. Francois, "Energy management and operational planning of a microgrid with a pv-based active generator for smart grid applications," *IEEE Transactions on Industrial Electronics*, vol. 58, pp. 4583–4592, Oct 2011.

[7] Y. Moumouni, Y. Baghzouz, and R. Boehm, "Power smoothing of a commercial-size photovoltaic system by an energy storage system," in *2014 IEEE 16th International Conference on Harmonics and Quality of Power (ICHQP)*, pp. 640–644, May 2014.

[8] M.-S. Lu, C.-L. Chang, W.-J. Lee, and L. Wang, "Combining the wind power generation system with energy storage equipment," *IEEE Transactions on Industry Applications*, vol. 45, pp. 2109–2115, Nov 2009.

[9] J. Cui, K. Li, Y. Sun, Z. Zou, and Y. Ma, "Distributed energy storage system in wind power generation," in *2011 4th International Conference on Electric Utility Deregulation and Restructuring and Power Technologies (DRPT)*, pp. 1535–1540, July 2011.

[10] W. Li and G. Joos, "Performance comparison of aggregated and distributed energy storage systems in a wind farm for wind power fluctuation suppression," in *Power Engineering Society General Meeting, 2007. IEEE*, pp. 1–6, June 2007.

[11] F. Marra, G. Yang, C. Traeholt, J. Ostergaard, and E. Larsen, "A decentralized storage strategy for residential feeders with photovoltaics," *IEEE Transactions on Smart Grid*, vol. 5, pp. 974–981, March 2014.

[12] H. Beltran, E. Bilbao, E. Belenguer, I. Etxeberria-Otadui, and P. Rodriguez, "Evaluation of storage energy requirements for constant production in pv power plants," *Industrial Electronics, IEEE Transactions on*, vol. 60, pp. 1225–1234, March 2013.

[13] Y. Zhang, H. J. Jia, and L. Guo, "Energy management strategy of islanded microgrid based on power flow control," in *Innovative Smart Grid Technologies (ISGT), 2012 IEEE PES*, pp. 1–8, 2012.

[14] I. S. C. C. 21, "Ieee guide for optimizing the performance and life of lead-acid batteries in remote hybrid power systems," 2008.
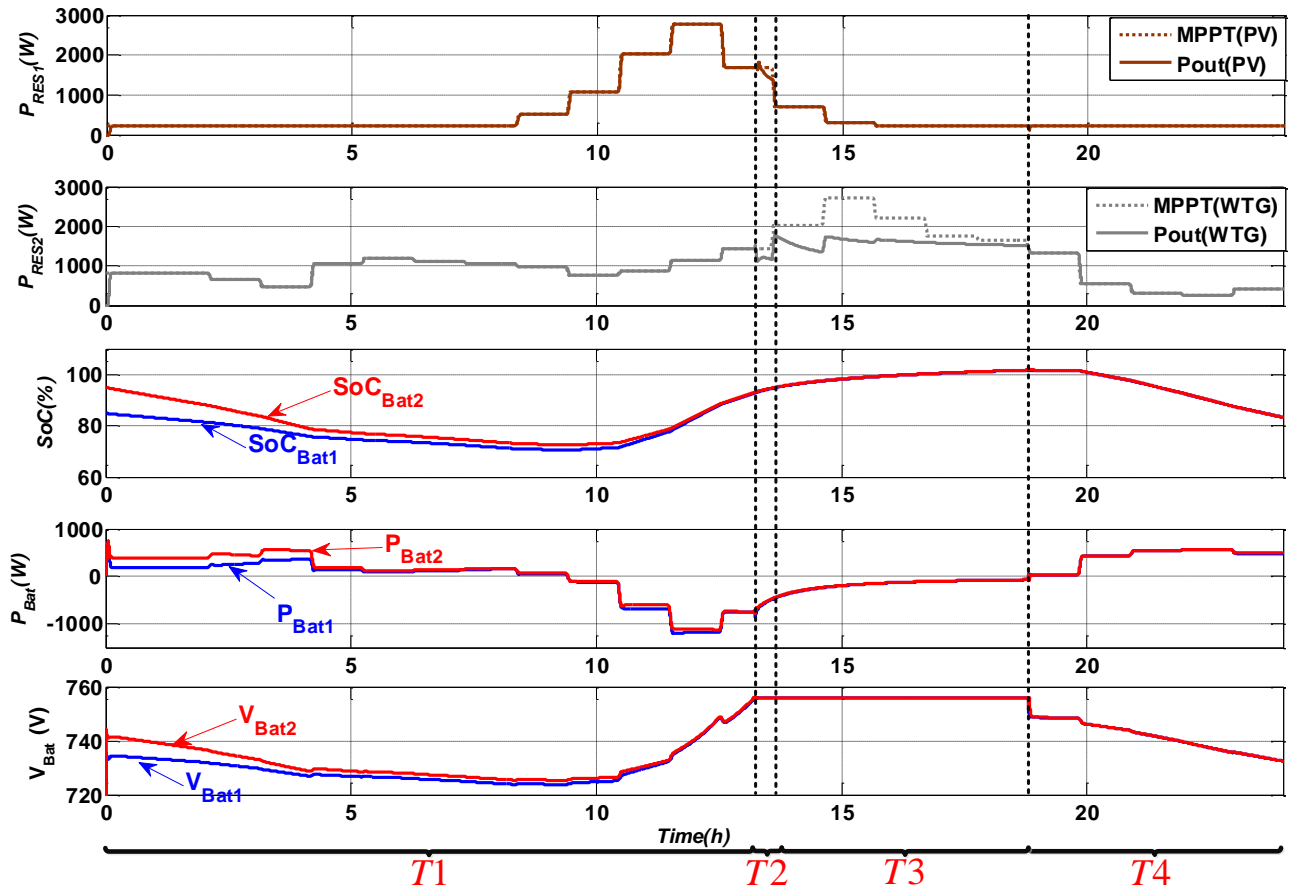
Figure 10: Islanded (PV+ESS) plus (WTG+ESS) microgrid operation for 24 hours.

[15] T. Dragicevic, J. Guerrero, J. Vasquez, and D. Skrlec, "Super-visory control of an adaptive-droop regulated dc microgrid with battery management capability," *IEEE Transactions on Power Electronics*, vol. 29, no. 2, pp. 695–706, 2014.

[16] N. Diaz, T. Dragicevic, J. Vasquez, and J. Guerrero, "Intelligent distributed generation and storage units for dc microgrids - a new concept on cooperative control without communications beyond droop control," *IEEE Transactions on Smart Grid*, vol. 5, pp. 2476–2485, Sept 2014.

[17] Y.-K. Chen, Y.-C. Wu, C.-C. Song, and Y.-S. Chen, "Design and implementation of energy management system with fuzzy control for dc microgrid systems," *Power Electronics, IEEE Transactions on*, vol. 28, no. 4, pp. 1563–1570, 2013.

[18] J. Guerrero, J. Vasquez, J. Matas, M. Castilla, and L. de Vicuna, "Control strategy for flexible microgrid based on parallel line-interactive ups systems," *IEEE Transactions on Industrial Electronics*, vol. 56, no. 3, pp. 726–736, 2009.

[19] X. Lu, K. Sun, J. Guerrero, J. Vasquez, L. Huang, and R. Teodorescu, "Soc-based droop method for distributed energy storage in dc microgrid applications," in *Industrial Electronics (ISIE), 2012 IEEE International Symposium on*, pp. 1640–1645, 2012.

[20] H. Kakigano, Y. Miura, and T. Ise, "Distribution voltage control for dc microgrids using fuzzy control and gain-scheduling technique," *Power Electronics, IEEE Transactions on*, vol. 28, no. 5, pp. 2246–2258, 2013.

[21] C. Li, T. Dragicevic, N. Diaz, J. Vasquez, and J. Guerrero, "Voltage scheduling droop control for state-of-charge balance of distributed energy storage in dc microgrids," in *Energy Conference (ENERGYCON), 2014 IEEE International*, pp. 1310–1314, May 2014.

[22] C. Li, T. Dragicevic, M. G. Plaza, F. Andrade, J. C. Vasquez, and J. M. Guerrero, "Multiagent based distributed control

for state-of-charge balance of distributed energy storage in dc microgrids," in *Industrial Electronics Society, IECON 2014 - 40th Annual Conference of the IEEE*, pp. 2180–2184, Oct 2014.

[23] X. Lu, K. Sun, J. Guerrero, J. Vasquez, and L. Huang, "State-of-charge balance using adaptive droop control for distributed energy storage systems in dc microgrid applications," *IEEE Transactions on Industrial Electronics*, vol. 61, pp. 2804–2815, June 2014.

[24] X. Lu, K. Sun, J. Guerrero, J. Vasquez, and L. Huang, "Double-quadrant state-of-charge-based droop control method for distributed energy storage systems in autonomous dc microgrids," *Smart Grid, IEEE Transactions on*, vol. 6, pp. 147–157, Jan 2015.

[25] Q. Shafiee, T. Dragicevic, J. Vasquez, and J. Guerrero, "Hierarchical control for multiple dc-microgrids clusters," *Energy Conversion, IEEE Transactions on*, vol. 29, pp. 922–933, Dec 2014.

[26] J. Rocabert, A. Luna, F. Blaabjerg, and P. Rodri?guez, "Control of power converters in ac microgrids," *IEEE Transactions on Power Electronics*, vol. 27, pp. 4734–4749, Nov 2012.

[27] J. Guerrero, L. Garcia De Vicuna, J. Matas, M. Castilla, and J. Miret, "A wireless controller to enhance dynamic performance of parallel inverters in distributed generation systems," *IEEE Transactions on Power Electronics*, vol. 19, pp. 1205–1213, Sept 2004.

[28] Y. Zhang, H. J. Jia, and L. Guo, "Energy management strategy of islanded microgrid based on power flow control," in *2012 IEEE PES Innovative Smart Grid Technologies (ISGT)*, pp. 1–8, Jan 2012.

[29] D. Linden and T. Reddy, *Handbook of batteries*. McGraw-Hill handbooks, McGraw-Hill, 2002.

[30] R. Babuska, *Fuzzy and Neuronal Control, Course Lecture Notes*. Delft University of Technology, 2009.